Fast Chebyshev-polynomial method for simulating the time evolution of linear dynamical systems

Y. L. Loh,[1] S. N. Taraskin,[2] and S. R. Elliott[2]
[1]*Trinity College, University of Cambridge, Cambridge CB2 1TQ, United Kingdom*
[2]*Department of Chemistry, University of Cambridge, Lensfield Road, Cambridge CB2 1EW, United Kingdom*

(Received 27 January 2000; revised manuscript received 5 December 2000; published 26 April 2001)

We present a fast method for simulating the time evolution of any linear dynamical system possessing eigenmodes. This method does not require an explicit calculation of the eigenvectors and eigenfrequencies, and is based on a Chebyshev polynomial expansion of the formal operator matrix solution in the eigenfrequency domain. It does not suffer from the limitations of ordinary time-integration methods, and can be made accurate to almost machine precision. Among its possible applications are harmonic classical mechanical systems, quantum diffusion, and stochastic transport theory. An example of its use is given for the problem of vibrational wave-packet propagation in a disordered lattice.

DOI: 10.1103/PhysRevE.63.056706 PACS number(s): 02.60.Cb, 02.70.Ns, 02.70.−c

I. INTRODUCTION

Consider a dynamical system evolving in time, and suppose that the time-evolution problem can be reduced to the eigenvalue-eigenvector problem. If the eigenvalues and corresponding eigenvectors are known, then all dynamical variables describing the system can be found at any moment of time. Let us suppose that the eigenvalues and eigenvectors of the system exist but cannot be found either analytically or numerically, e.g., because the number of variables involved is very large. The question is this: Can we predict (calculate or simulate) the dynamical state of the system at any moment of time knowing only its equations of motion, the initial boundary conditions, and the fact that the system can be characterized by the eigenvalues and eigenvectors? The answer is yes (obvious in the case of the existence of an analytical solution). The standard way, though rather inefficient, is to solve the equations of motion by a numerical integration scheme. This usually involves performing a large number of integration time steps to reach the desired moment of time (see, e.g., Ref. [1]). Such schemes are applicable to general dynamical systems which are not necessarily described by eigenfunctions and eigenvalues, but do not take advantage of the existence of eigenfunctions and eigenvalues where they are available.

In this paper, we suggest a general, numerically efficient approach for the solution of time-evolution problems for dynamical systems, particularly involving second-order differential equations, which can be described by eigenfunctions and eigenvalues [2,3]. Our approach is quite the opposite of time-integration schemes, which treat the problem in the time domain by sampling the time continuum at discrete intervals. Instead, we solve the time-evolution problem in the frequency (or eigenvalue) domain, taking advantage of the fact that each eigenvector evolves independently of the others. This allows us to find all dynamical variables at any moment of time after, in fact, only one time step. This approach is applicable to a broad class of dynamical systems, the interactions in which are described by linear Hermitian operators, and the time-evolution operator can be of quite general form. For example, quantum-mechanical systems characterized by time-independent Hamiltonians and classical harmonic atomic systems described by dynamical matrices can be treated by the method developed below. Among the physical problems to which this fast evolution method (FEM) can be applied are stochastic transport theory [4], quantum diffusion and electron localization problems [5,6], wave propagation in disordered atomic structures [7,8] etc.

The basic idea behind the FEM is to expand the formal (operator) solution of the problem in a series of suitable (Chebyshev) polynomials defined on the set of operators. The coefficients in such expansions depend only on time and on the form of the time-evolution operator, and possibly on external sources or forces; they are independent of the number of dynamical variables and the form of the interaction operator. This provides the generality of the approach. In fact, the FEM was inspired by several ideas: (i) the possibility of using higher-order integration algorithms [1]; (ii) the kernel polynomial method developed by Silver and Röder [9] for the calculations of density of states and other spectral functions for large systems; and (iii) the unstable-oscillator method of Okamoto and Maris [10], which employs an unusually large integration time step for calculations of the extreme eigenvalues and eigenvectors. Chebyshev-polynomial-based propagator methods have been extensively used to study the time evolution of quantum systems obeying the (first-order differential) time-dependent Schrödinger equation [11]—see Refs. [12–14]. However, to the best of our knowledge, they have not been used for an investigation of the time evolution of, e.g., atomic vibrational problems involving the solution of second-order differential equations. This is the subject of this paper.

The computational efficiency of the FEM is due to the fact that the polynomials defined in terms of operators can be easily computed in the matrix representation of the operators. The FEM has very reasonable time and space requirements, can give an extremely high accuracy, and is easily vectorized. It is especially useful for large systems, e.g., with $\sim 10^7$ atoms characterized by sparse matrices, in which case the computation time scales linearly with the number of coordinates as well as with the evolution time.

The rest of the paper is arranged in the following manner.

Section II briefly outlines the problem; the formal solution is presented in Sec. III, and the Chebyshev polynomial expansion, which is the basis of the FEM, is described in Sec. IV. The widely used Verlet algorithm is analyzed in Sec. V, and in Sec. VI we put forth an improved Verlet algorithm (which unfortunately did not entirely live up to our hopes). The results of tests of the computational performance of the FEM for the case of vibrations of an ordered linear chain of atoms are presented in Sec. VII. A representative application of the FEM, to the case of wave-packet propagation in disordered three-dimensional media, is given in Sec. VIII. Details of the calculation of the coefficients in the Chebyshev series are given in the Appendix.

II. FORMULATION OF THE PROBLEM

Let us consider a dynamical system, the state of which can be characterized by a state vector $|\mathbf{u}\rangle \equiv \mathbf{u}$ in a linear vector space of dimensionality N spanned by the orthonormal basis $\{\mathbf{s}_i\}$ $(i=1,\ldots,N)$. Suppose that the state of the system evolves with time $\mathbf{u}(t)$ according to the equation of motion

$$\hat{\mathbf{T}}(t)\mathbf{u}(t)+\hat{\mathbf{H}}\mathbf{u}(t)=\mathbf{0}, \tag{1}$$

with $\hat{\mathbf{T}}(t)$ being a time-evolution operator and $\hat{\mathbf{H}}$ being the time-independent linear Hermitian operator responsible for interactions and defined in the same linear vector space. The operator $\hat{\mathbf{H}}$ can be written in the matrix form $\mathbf{H}^s$, with the elements $H^s_{ij}=\langle \mathbf{s}_i|\hat{\mathbf{H}}|\mathbf{s}_j\rangle$ calculated, e.g., in the basis $\{\mathbf{s}_i\}$. The state vector $\mathbf{u}$ can also be characterized by its components (projections) in the same basis, $\mathbf{u}\{\mathbf{u}^s_1,\ldots,\mathbf{u}^s_N\}$. The matrix $\mathbf{H}^s$ is not necessarily diagonal in the $\mathbf{s}$ representation, but there is a unitary transformation $\hat{\mathbf{E}}$ to the orthonormal basis $\{\mathbf{e}_i\}$ (the eigenvector basis), in which the matrix $\mathbf{H}^e$ is diagonal (see, e.g., Ref. [15]). The standard expressions connecting the vectors and matrices in different representations are: $\mathbf{u}^e=\mathbf{E}^{-1}\mathbf{u}^s$ and $\mathbf{H}^e=\mathbf{E}^{-1}\mathbf{H}^s\mathbf{E}$, with the matrix $\mathbf{E}$ containing the eigenvectors $\mathbf{e}_i$ (with the corresponding eigenvalues λ_i) as the columns in the $\mathbf{s}$ representation.

The time-evolution operator could be a quite general integrodifferential time-dependent operator. What is important for us is just the fact that the solution, $\mathbf{u}(t,\lambda)$, of Eq. (1), in which the operator $\hat{\mathbf{H}}$ is replaced by a scalar number λ (e.g., one of the eigenvalues of the matrix $\mathbf{H}$),

$$\hat{\mathbf{T}}(t)\mathbf{u}(t,\lambda)=\lambda\mathbf{u}(t,\lambda), \tag{2}$$

exists, and can be found for certain initial conditions, either analytically or numerically. If this is the case, we assume that the formal solution of Eq. (1) also exists, and can be written as $\mathbf{u}(t,\mathbf{H})$. One of the simplest realizations for the operator $\hat{\mathbf{T}}(t)$ is a linear differential operator in the form

$$\hat{\mathbf{T}}(t)=\alpha_2(t)\frac{\partial^2}{\partial t^2}+\alpha_1(t)\frac{\partial}{\partial t}+\alpha_0(t), \tag{3}$$

with $\alpha_n(t)$ being functions of time.

There are two straightforward important physical applications for Eqs. (1)–(3). The first one is for the case $\alpha_2(t)=1$ and $\alpha_1(t)=\alpha_0(t)=0$ in Eq. (3), so that Eq. (1) can be rewritten in the form

$$\ddot{\mathbf{u}}+\mathbf{H}\mathbf{u}=\mathbf{0}. \tag{4}$$

This is the equation of motion of a classical harmonic mechanical system of N_a particles without friction in a D-dimensional $(N=DN_a)$ real space (system of N_a coupled harmonic oscillators). In that case, the $\mathbf{s}$ basis can be the site basis, with the basis vector being a unit displacement vector (from the equilibrium position) of one of the particles (atoms) along one of the Cartesian axes. The vector $\mathbf{u}^s$ is then the mass-weighted (multiplied by the square root of the atomic mass) displacement vector, and $\mathbf{H}^s$ is the dynamical matrix containing the second derivatives of the potential energy [16]. The initial conditions for such a problem are usually defined by the atomic positions and velocities:

$$\mathbf{u}(t=0)=\mathbf{u}_0, \tag{5}$$

$$\dot{\mathbf{u}}(0)=\mathbf{v}_0. \tag{6}$$

Equations (4)–(6) provide a complete description of the dynamical system.

The second obvious application is for $\alpha_2(t)=\alpha_0(t)=0$, $\alpha_1(t)=-i$ in Eq. (3), so that the equation of motion looks like

$$i\frac{\partial}{\partial t}\boldsymbol{\Psi}=\mathbf{H}\boldsymbol{\Psi}. \tag{7}$$

This is just the particular case of the Schrödinger equation $(\hbar=1)$, where the vector $\mathbf{u}$ is replaced by the wave function state vector $\boldsymbol{\Psi}$ defined in the finite-dimensional linear space. The $\mathbf{s}$ basis can be any suitable finite basis (e.g., the site basis for solid-state tight-binding Hamiltonians [17]). The matrix $\mathbf{H}$ is the Hamiltonian matrix defined in the same basis, with elements $H^s_{ij}=\langle \mathbf{s}_i|\hat{\mathbf{H}}|\mathbf{s}_j\rangle$. For example, it could be the Anderson Hamiltonian in the site basis [5], or a perturbed Hamiltonian in the finite basis of the non-perturbed one [15], etc. The initial condition for such a problem could be

$$\boldsymbol{\Psi}(0)=\Psi_0. \tag{8}$$

Equations (7) and (8) describe the evolution of a quantum-mechanical system with time. The classical one-dimensional lattice-vibrational problem is equivalent to the quantum problem of an electron propagating along a chain of atoms, each with a single orbital [18].

Our main task here is to find the solution of the problem given by Eq. (1) for a certain class of operators $\hat{\mathbf{H}}$ (linear, Hermitian, and defined in the vector space spanned by a finite orthonormal basis) and $\hat{\mathbf{T}}$ [the existence of the solution of the auxiliary equation (2) is required] for an arbitrary time t, assuming the corresponding initial conditions and matrix elements of the operator $\mathbf{H}$ to be known. In what follows, we pay more attention to the classical problem described by Eqs.

(4)–(6), bearing in mind that the quantum problem [Eqs. (7) and (8)] can be treated similarly [12–14].

III. FORMAL SOLUTION

Let us consider, for definiteness, an equation of motion in the form which includes the two important physical applications discussed in Sec. II,

$$\alpha_2\ddot{\mathbf{u}}+\alpha_1\dot{\mathbf{u}}+(\alpha_0+\mathbf{H})\mathbf{u}=\mathbf{0}, \tag{9}$$

with α_i being constants. The initial conditions for Eq. (9) are given by Eqs. (5) and (6). The solution of this problem can be trivially found in the eigenvector basis,

$$\mathbf{u}(t)=A(\mathbf{H};t)\mathbf{u}_0+B(\mathbf{H};t)\mathbf{v}_0, \tag{10}$$

with the matrix functions

$$A(\mathbf{H};t)=\frac{\exp\{i\omega_1(\mathbf{H})t\}-\exp\{i\omega_2(\mathbf{H})t\}}{i(\omega_1(\mathbf{H})-\omega_2(\mathbf{H}))}, \tag{11}$$

$$B(\mathbf{H};t)=\frac{-\omega_2(\mathbf{H})\exp\{i\omega_1(\mathbf{H})t\}+\omega_1(\mathbf{H})\exp\{i\omega_2(\mathbf{H})t\}}{\omega_1(\mathbf{H})-\omega_2(\mathbf{H})}. \tag{12}$$

The frequencies $\omega_1(\mathbf{H})$ and $\omega_2(\mathbf{H})$ obey the equation

$$\omega_{1,2}(\mathbf{H})=\frac{1}{2\alpha_2}\{i\alpha_1\mathbf{I}\pm\sqrt{-\alpha_1^2\mathbf{I}+4\alpha_2(\alpha_0\mathbf{I}-\mathbf{H})}\}, \tag{13}$$

with $\mathbf{I}$ being the unit matrix. One of the useful realizations of these general expressions is for the classical harmonic vibrational problem characterized by $\alpha_2=1$ and $\alpha_1=\alpha_0=0$ and described by the equation of motion (4). In this particular case, $\omega_{1,2}(\mathbf{H})=\pm i\sqrt{\mathbf{H}}$, so that

$$A(\mathbf{H};t)=\cos\sqrt{\mathbf{H}}t, \tag{14}$$

$$B(\mathbf{H};t)=\mathbf{H}^{-1/2}\sin\sqrt{\mathbf{H}}t, \tag{15}$$

with the spectrum of the matrix $\mathbf{H}$ lying in the interval $\lambda\in[0,\lambda_{\max}]$.

This is a standard approach to the problem given by Eq. (1), which assumes a knowledge of the eigenvalues and eigenvectors of the problem. In some special cases, e.g., for symmetric dynamical matrices describing crystals, the eigenvalues and eigenvectors can be solved analytically, but in the general case the analytical solution is not known and the eigenvalues and eigenvectors are available only numerically. A direct diagonalization of the matrix $\mathbf{H}$ (which could be dense) is possible for $N\lesssim10^4$. Approximate methods (e.g., Lanczos [19]) allow sparse matrices with $N\lesssim10^6$ to be solved, but normally either only the eigenvalues and/or the eigenvectors from a restricted range of the spectrum are available (see, e.g., Refs. [20,21]). The calculation of all eigenvalues and eigenvectors for large sparse matrices ($N\lesssim10^6$) is possible in principle, but requires a lot of computational effort (time and memory).

The key point of our approach is to avoid the calculations of eigenvalues and eigenvectors but to assume their existence only, i.e., the existence of the formal solution [Eqs. (10)–(13)] in the eigenvector basis. This formal solution is actually independent of the basis and valid for any, e.g., site, representation of matrix $\mathbf{H}$ and displacement vectors $\mathbf{u}$ [this can be easily shown by applying a linear transformation to a new basis, Eq. (10), and that is why the basis superscript is omitted in Eqs. (10)–(15)]. Therefore, we can use the formal solution exactly in that basis in which the $\mathbf{H}$ matrix and initial vectors are available. This is not a straightforward procedure, because the matrix $\mathbf{H}$ is not necessarily diagonal in the available basis, so that the functions $A(\mathbf{H};t)$ and $B(\mathbf{H};t)$ in Eq. (10) should be understood in terms of a power series of matrix $\mathbf{H}$. The question of how to choose the most convenient expansions for $A(\mathbf{H};t)$ and $B(\mathbf{H};t)$ is discussed in detail below.

One of the other possible known ways not to use the eigenvalues and eigenvectors lies in the time-integration schemes for Eq. (1), the most popular of them probably being the Verlet method [1] for the atomic dynamics problem [Eq. (4)]. The drawback of this and similar approaches is the small integration time step which is necessary to obtain an accurate solution, and therefore the long computational times required in order to evolve the system quite far from its initial conditions (see, e.g., Refs. [1,18,20,22,23]). Moreover, the standard integration schemes are quite general (e.g., applicable for nonlinear operators $\hat{\mathbf{H}}$), and do not use the fact of the existence of the eigenvalues and eigenvectors, making them not very efficient for the system under consideration. Below, we develop a fast time-evolution method which is free of such drawbacks, and which allows the time evolution of the system to be calculated without small integration time steps, and even to jump to the final state (using only one ''integration'' step) at a time t which is far away from the initial moment t_0, e.g., $\omega_{\max}(t-t_0)\gtrsim10^4$, with $\omega_{\max}$ being the maximum eigenfrequency of the system.

IV. CHEBYSHEV POLYNOMIAL EXPANSION

In Sec. III, we found the formal solution [Eqs. (10)–(13)] of the problem given by Eq. (9) with initial conditions given by Eqs. (5) and (6) which allows, in principle, the state vector $\mathbf{u}(t)$ to be calculated at any moment of time. In order to do this in practice, we have to specify the way how to manipulate the functions $A(\mathbf{H};t)$ and $B(\mathbf{H};t)$ defined with matrix arguments. The most straightforward way, on which the time-integration schemes are based, is to expand these functions in a Taylor series around $t=0$. The series can be evaluated by a sequence of matrix-vector multiplications. This is accurate for small values of $\omega_{\max}t\lesssim1$, but for $\omega_{\max}t\gtrsim10-10^2$ the inherent instability in the process of Taylor expansion results in cancellations between successive terms and a complete loss of precision.

An alternative way is based on an expansion in the eigenfrequency domain. Let us treat t as a parameter, and $\mathbf{H}$ as a matrix variable in the functions $A(\mathbf{H};t)$ and $B(\mathbf{H};t)$. These functions can then be expanded in a series of an appropriate complete set of functions $\phi_p(\mathbf{H})$ with time-dependent coefficients. The choice of the basis set for the expansion is dictated by the following requirements: the functions $\phi_p(\mathbf{H})$

should preferably be polynomials, since evaluating matrix polynomials requires only simple matrix operations; the functions $\phi_p(\mathbf{H})$ need to form a complete set only over a finite interval because the spectrum of $\mathbf{H}$ is bounded; and the coefficients in the expansion should be fast and easy to compute. All these requirements are met by the Chebyshev polynomials [9], $T_p(\mathbf{H}')=\cos(p\cos^{-1}\mathbf{H}')$, which form a complete set for the matrix $\mathbf{H}'$ if its eigenvalue spectrum is confined to the interval $[-1,1]$; they are defined by the following recurrence relations:

$$T_0(\mathbf{H}')=\mathbf{I}, \tag{16}$$

$$T_1(\mathbf{H}')=\mathbf{H}', \tag{17}$$

$$T_{p+1}(\mathbf{H}')=2\mathbf{H}'T_p(\mathbf{H}')-T_{p-1}(\mathbf{H}'). \tag{18}$$

In order to use the standard Chebyshev polynomials, first we map the spectrum, $\lambda_i\in[\lambda_{\min},\lambda_{\max}]$ of the matrix $\mathbf{H}$ onto the interval $[-1,1]$ by the following linear transformation:

$$\mathbf{H}'=\frac{2\mathbf{H}-(\lambda_{\max}+\lambda_{\min})\mathbf{I}}{\lambda_{\max}-\lambda_{\min}}. \tag{19}$$

The upper and lower bounds $\lambda_{\max}$ and $\lambda_{\min}$ to its spectrum can be easily estimated by different methods, e.g., by the Gerschgorin circle theorem [19].

The functions $A(\mathbf{H};t)$ and $B(\mathbf{H};t)$ can then be expanded as sums of Chebyshev polynomials of the new matrix $\mathbf{H}'$:

$$A(\mathbf{H};t)=\sum_{p=0}^{\infty}a_p(t)T_p(\mathbf{H}'), \tag{20}$$

$$B(\mathbf{H};t)=\sum_{p=0}^{\infty}b_p(t)T_p(\mathbf{H}'). \tag{21}$$

The coefficients $a_p(t)$ and $b_p(t)$ for the desired evolution time t can be easily found using the orthogonality of the Chebyshev polynomials and fast Fourier transformation (FFT) methods (see the Appendix). The coefficients are independent of the concrete form of the matrix $\mathbf{H}$ (only the spectral bounds $\lambda_{\max}$ and $\lambda_{\min}$ enter the expressions for them), and are defined mainly by the form of the time-evolution operator $\hat{\mathbf{T}}$, i.e., by the concrete form of the functions $A(\mathbf{H};t)$ and $B(\mathbf{H};t)$. This ensures the generality of the method.

Once the coefficients $a_p(t)$ and $b_p(t)$ are found, the solution for the state vector at an arbitrary time t can be written as follows:

$$\mathbf{u}(t)=\left(\sum_{p=0}^{P-1}a_p(t)T_p(\mathbf{H}')\right)\mathbf{u}_0+\left(t\sum_{p=0}^{P-1}b_p(t)T_p(\mathbf{H}')\right)\mathbf{v}_0. \tag{22}$$

This expression is the solution of the problem and is a key point of the FEM. We should stress that the polynomials $T_p(\mathbf{H}')$ actually enter into solution (22) as products with the initial vectors $\mathbf{u}_0$ and $\mathbf{v}_0$. This fact significantly improves the computational performance, so that for a sparse matrix $\mathbf{H}$ the computing time scales linearly with the number of variables $O(N)$.

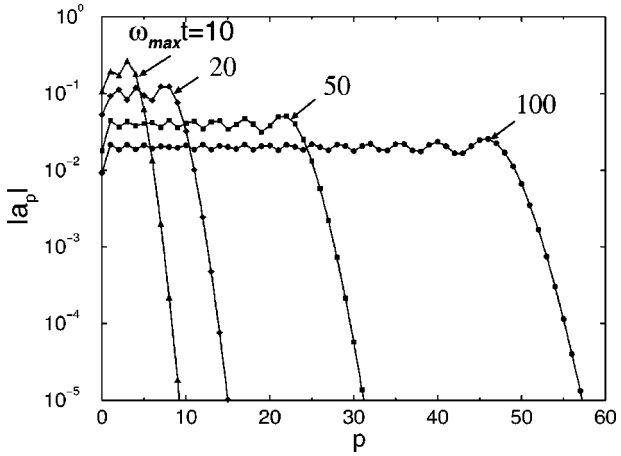

FIG. 1. The magnitude of the expansion coefficients, $|a_p|$, in Eq. (20) vs the order p of the Chebyshev polynomials for different evolution times t as indicated (with $\omega_{\max}=2$ as for a $1D$ ideal atomic linear chain model).

The infinite limits in the series in Eqs. (20) and (21) have been replaced in Eq. (22) by finite values $P-1$ for the maximum order of the polynomials. In order to assess the validity of this, we have investigated the dependence of the magnitude of the coefficients a_p and b_p on the polynomial order p in the case of the classical harmonic vibrational problem characterized by functions $A(\mathbf{H};t)$ and $B(\mathbf{H};t)$ given by Eqs. (14) and (15). It appears that, at fixed t, the coefficients a_p and b_p first oscillate with increasing p and then decay exponentially with further increase of p (see Fig. 1 for the choice of parameters appropriate to the particular case of a linear harmonic atomic chain). Such a behavior of the coefficients a_p and b_p with p allows us to truncate the series in Eq. (21) at a certain order P of the polynomials such that the contribution from succeeding terms is negligible. A suitable truncation condition is

$$\max\{|a_P(t)|,|b_P(t)|\}=\varepsilon, \tag{23}$$

with ε being the error bound. As a_p and b_p decay roughly exponentially for $p>P$ with a typical scale $\delta_P\sim 1$ (see Fig. 1), the rest of the series can be estimated to be not greater than $\varepsilon\,\delta_P$.

Condition (23) can be solved for the optimal number of Chebyshev terms, P. The value of P depends on $\omega_{\max}t$ (with $\omega_{\max}=\sqrt{\lambda_{\max}}$) and on the tolerance ε. The behavior of $P(\omega_{\max}t)$ for different ε is shown in Fig. 2. For practical use, these curves can be approximated by the empirical expression

$$P(\sqrt{\lambda_{\max}}t|\varepsilon)\simeq-\alpha(\varepsilon)\ln(\varepsilon)+\beta(\varepsilon)(\sqrt{\lambda_{\max}}t)+\gamma(\varepsilon)(\sqrt{\lambda_{\max}}t)^{\delta(\varepsilon)}, \tag{24}$$

with the parameters $\alpha(\varepsilon)$, $\beta(\varepsilon)$, $\gamma(\varepsilon)$, and $\delta(\varepsilon)$ depending slightly on ε [see Figs. 3(a) and 3(b)]. The number of poly-

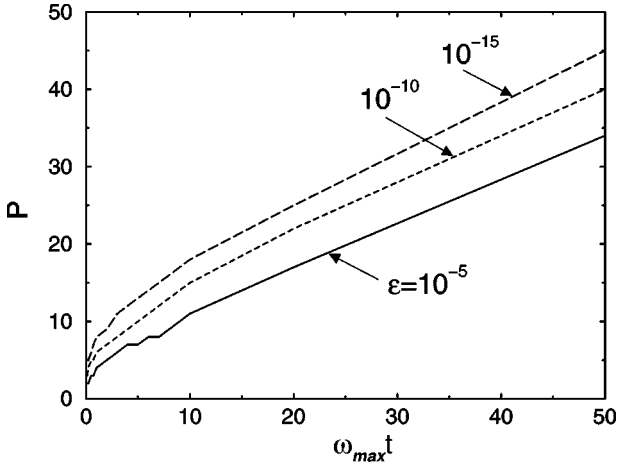

FIG. 2. The number of Chebyshev polynomials used, P, against the product $\omega_{\max}t$, for different error bounds ϵ. For small $\omega_{\max}t$, the graph is nonlinear, but as $\omega_{\max}t\to\infty$, P becomes approximately proportional to $\omega_{\max}t$. Increasing ϵ has the effect of increasing P by a roughly constant amount.

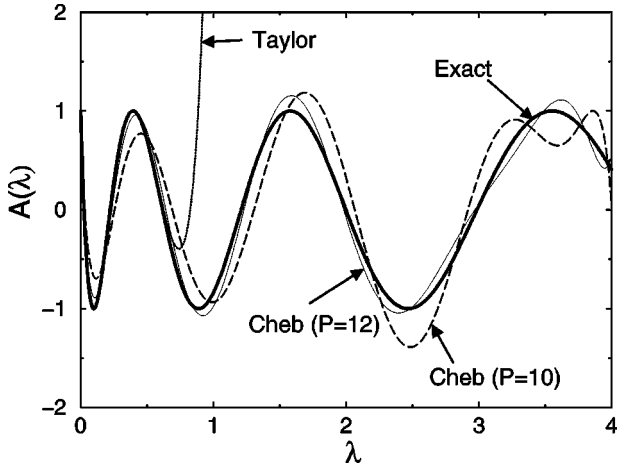

FIG. 4. The ''time evolution function'' $A(\lambda)=\cos\sqrt{\lambda}t$ (thick solid line) and its approximation by ten- ($P=10$) (dashed line) and 12-term ($P=12$) (thin solid line) Chebyshev series, and by an 11-term Taylor series [terms up to λ^{10} (dotted line)] for $t=10$ and $\lambda_{\max}=4$.

nomials P used in the expansion not surprisingly grows with time, and the maximum order of the polynomials (number of roots of the polynomial) can be estimated as the number of oscillations with a typical frequency $\omega_*=\sqrt{\lambda_*}$ in time t, i.e.,

$$P\simeq\omega_* t/\pi \quad \text{for } P\gg 1. \tag{25}$$

The typical frequency is normally of the same order as the maximum frequency, $\omega_*=\chi\omega_{\max}$, with $\chi\sim 1$. In the case of a linear chain, the value of χ is roughly $\chi\simeq\beta(\varepsilon)\pi\simeq 1.6$; see Fig. 3(a). The computational time for the coefficients a_p and b_p scales as $O(P\log_2 P)$ and is negligible in comparison with the matrix-vector multiplication time (see below).

In order to illustrate how the Chebyshev expansion fits solution (10), we calculated the Chebyshev series (the dashed curve in Fig. 4) for the function $A(\lambda)=\cos\sqrt{\lambda}t$ [see Eq. (14)] entering the solution, and compared it with the known exact behavior (see the solid curve in Fig. 4) for the particular values $t=20$ and $\lambda_{\max}=4$. As seen from Fig. 4, the Chebyshev expansion with $P=10$ polynomials mainly reproduces the shape of the function $\cos\sqrt{\lambda}t$ in the whole eigenvalue range. For $P=12$ the agreement is much better (see the thin solid line in Fig. 4), and for $P=15$ the difference between the Chebyshev expansion and the exact function is not seen by eye ($P=25$ is more appropriate for practical use; also see Fig. 2). The Taylor expansion can also be used to fit this function. Keeping the terms up to $O(\lambda^{10})$ (which requires the same computational time as for the Chebyshev expansion), we obtained the dotted curve in Fig. 4. This clearly shows that the Taylor expansion is accurate at small λ but diverges catastrophically for larger λ. In contrast, the error in the Chebyshev approximation is spread uniformly over the whole spectrum. This demonstrates the superiority of the Chebyshev approximation over the Taylor series.

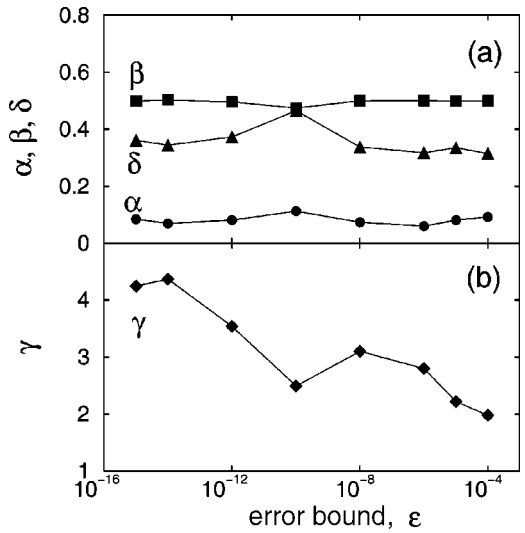

FIG. 3. The dependence of the coefficients α, β, γ, and δ, in the empirical equation (24), for the maximum number of Chebyshev polynomials P on the error bound ϵ. The lines are guides for the eye.

The FEM can be easily generalized for the classical harmonic vibrational system [see Eq. (4)] subject to an external force field, $\mathbf{H}^{\text{ext}}(\mathbf{R}_i,t)$, with $\mathbf{R}_i$ characterizing an equilibrium position of atom i, so that Eq. (4), can be rewritten as

$$\ddot{\mathbf{u}}+\hat{\mathbf{H}}\mathbf{u}=\hat{\mathbf{C}}\mathbf{H}^{\text{ext}}(\mathbf{R}_i,t), \tag{26}$$

with $\hat{\mathbf{C}}$ being a coupling operator described by a coupling matrix $\mathbf{C}$ of the external field with the system. In the case of the electromagnetic field, for example, this matrix contains atomic charges. If the interactions are local, then the $\mathbf{C}$ matrix contains nonzero elements mainly around the diagonal, while in the case of nonlocal interactions the nonzero elements can be distributed over the whole matrix. For definiteness, we consider an external field of the form

$$\mathbf{H}^{\text{ext}}(\mathbf{R}_i,t)=\sum_j \mathbf{f}_j^{\text{ext}}(\mathbf{R}_i)\exp\{\mathrm{i}\omega_j t\}, \tag{27}$$

with $\mathbf{f}_j^{\text{ext}}(\mathbf{R}_i)$ being time independent. Assuming the same initial conditions (5) and (6), it is straightforward to show that the formal general solution for the displacement vector is the sum of Eq. (10) and the particular integral, $\mathbf{u}_{\text{PI}}$,

$$\mathbf{u}_{\text{PI}}(t)=\sum_j \frac{1}{\mathbf{H}-\omega_j}\{\exp(\mathrm{i}\omega_j t)-\cos\sqrt{\mathbf{H}}t - \mathrm{i}\omega_j t\,\mathrm{sinc}\sqrt{\mathbf{H}}t\}\hat{\mathbf{C}}\mathbf{f}_j^{\text{ext}}(\mathbf{R}_i), \tag{28}$$

if none of the external frequencies ω_j coincides with any of the eigenfrequencies of the matrix $\mathbf{H}$ for the homogeneous problem, and

$$\mathbf{u}_{\text{PI}}(t)=\sum_j \frac{t}{2\mathrm{i}\sqrt{\mathbf{H}}}\{\exp(\mathrm{i}\sqrt{\mathbf{H}}t)-\mathrm{sinc}\sqrt{\mathbf{H}}t\}\hat{\mathbf{C}}\boldsymbol{f}_j^{\text{ext}}(\mathbf{R}_i) \tag{29}$$

otherwise. The particular integrals (28) and (29) can then be easily expanded in Chebyshev polynomials in a similar way to that described above for the homogeneous problem.

As mentioned above, the FEM can also be readily extended to the linear quantum-mechanical problem described by Eqs. (7) and (8), for which the formal solutions for $\boldsymbol{\Psi}(t)=\boldsymbol{\Psi}_u(t)+\mathrm{i}\boldsymbol{\Psi}_v(t)$ can be written as

$$\boldsymbol{\Psi}_u(t)=(\cos\mathbf{H}t)\boldsymbol{\Psi}_u(0)+(\sin\mathbf{H}t)\boldsymbol{\Psi}_v(0), \tag{30}$$

$$\boldsymbol{\Psi}_v(t)=-(\sin\mathbf{H}t)\boldsymbol{\Psi}_u(0)+(\cos\mathbf{H}t)\boldsymbol{\Psi}_v(0). \tag{31}$$

The functions $\cos\mathbf{H}t$ and $\sin\mathbf{H}t$ can then be easily expanded in Chebyshev polynomials in exactly the same way as above (also see Refs. [12–14]).

The fast evolution method can be also used as an elementary single-step calculation procedure in the integration algorithm, but the time step $t-t_0$ can be arbitrary. This means that the efficient integration method based on the Chebyshev polynomial expansion can be used to solve the equation of motion for the systems in question. It appears to be much faster and more accurate than other known schemes, e.g., the Verlet algorithm (see below).

V. VERLET ALGORITHM

An alternative way to use the formal solution [Eq. (10)] is to expand the functions entering it in a Taylor series, e.g., around $t=0$. For example, in the case of harmonic vibrations, the functions $(\cos\sqrt{\mathbf{H}}t)\mathbf{u}_0$ and $(\mathrm{sinc}\sqrt{\mathbf{H}}t)\mathbf{v}_0$ entering Eq. (10) [see Eqs. (14) and (15)] can be expanded as

$$(\cos\sqrt{\mathbf{H}}t)\mathbf{u}_0=\mathbf{u}_0-\frac{t^2}{2}\mathbf{H}\mathbf{u}_0+\frac{t^4}{24}\mathbf{H}^2\mathbf{u}_0, \tag{32}$$

$$(\mathrm{sinc}\sqrt{\mathbf{H}}t)\mathbf{v}_0=\mathbf{v}_0-\frac{t^2}{6}\mathbf{H}\mathbf{v}_0+\frac{t^4}{120}\mathbf{H}^2\mathbf{v}_0-\cdots. \tag{33}$$

The matrix-vector multiplications involved in Eqs. (32) and (33) make such an approach computationally efficient (especially for sparse matrices $\mathbf{H}$) at small t, when just a few (two or three) terms can be kept. The evolution with time can then be followed by step-by-step integration with the required number of steps to reach time t.

Therefore, the formal solution [Eq. (10)] can be represented as a polynomial in the matrix $\mathbf{H}$, and, in fact, all the time-integration schemes including the original Verlet algorithm and all its variants (e.g., high-order), Runge-Kutta algorithms and explicit predictor-corrector schemes (see, e.g., Ref. [1]) are based on it. For the sake of comparison with the FEM developed above, in this section we consider one of them, namely, the standard Verlet integration scheme applied to the evolution of classical harmonic systems.

For the system we have described above (e.g., harmonic atomic systems), the Verlet algorithm reads (see, e.g., Ref. [1])

$$\mathbf{u}_{j+1}=(2\mathbf{I}-\tau^2\mathbf{H})\mathbf{u}_j-\mathbf{u}_{j-1}, \tag{34}$$

where $\mathbf{u}_j$ is the displacement vector at time $t=j\tau$ for a time step j of length τ. This is actually a triple recurrence relation very similar to the Chebyshev polynomial recurrence [Eq. (18)].

Let us choose the displacement vector $\mathbf{u}(t)$ to be one of the eigenvectors of the system corresponding to the eigenfrequency $\omega=\sqrt{\lambda}$. In that case, we know exactly how it evolves with time, i.e., $\mathbf{u}(t)=\mathbf{C}_+\exp(\mathrm{i}\omega t)+\mathbf{C}_-\exp(-\mathrm{i}\omega t)$ where the constant vectors $\mathbf{C}_\pm$ are defined by the initial conditions. Then we can compare this exact solution with that obtained using the Verlet scheme. In order to find the solution of Eq. (34), first we replace the dynamical matrix $\mathbf{H}$ there by the corresponding eigenvalue λ. Then the general solution can be found in the form [10]

$$\mathbf{u}_j=\mathbf{C}_+(\mu_+)^j+\mathbf{C}_-(\mu_-)^j, \tag{35}$$

with $\mu_\pm$ obeying the equation

$$\mu_\pm=1-\frac{\theta^2}{2}\pm\mathrm{i}\left[1-\left(1-\frac{\theta^2}{2}\right)^2\right]^{1/2} \simeq 1\pm\mathrm{i}\theta-\frac{\theta^2}{2}\mp\frac{\mathrm{i}\theta^3}{8}+\cdots, \tag{36}$$

with $\theta=\sqrt{\lambda}\tau=\omega\tau$ and $|\mu_\pm|=1$. These values $\mu_\pm$ have to be compared with the exact solution

$$\mu_\pm^{\text{exact}}=\exp(\pm\mathrm{i}\omega\tau)\simeq 1\pm\mathrm{i}\theta-\frac{\theta^2}{2}\mp\frac{\mathrm{i}\theta^3}{6}+\frac{\theta^4}{24}\pm\frac{\mathrm{i}\theta^5}{120}\cdots. \tag{37}$$

As follows from a comparison of Eqs. (36) and (37) for small $\theta\ll 1$, the functions $\mu_\pm$ and $\mu_\pm^{\text{exact}}$ match up to the term in $O(\theta^2)$. This is an indication of the low-frequency and/or short-time accuracy of the Verlet algorithm. The gain error per step, being proportional to the deviation of the absolute value of μ from the unitary circle, is zero for the Verlet algorithm, because $|\mu_\pm|=1$; therefore, the energy is conserved for this scheme. On the other hand, the argument $\Theta_\pm$ of $\mu_\pm=|\mu_\pm|\exp(\mathrm{i}\Theta_\pm)$, defined by the equation

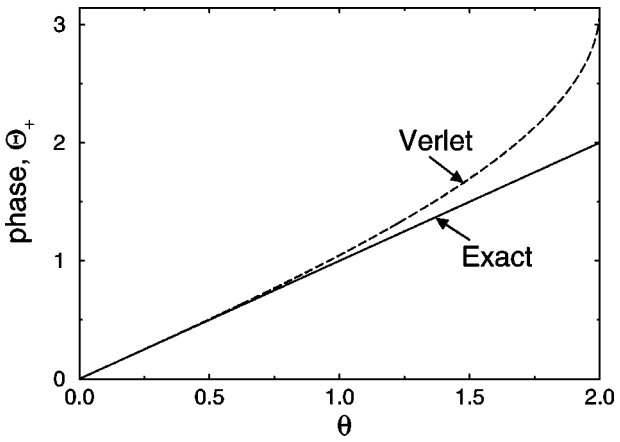

FIG. 5. The phase Θ_+ vs $\theta=\omega t$ for the exact solution $\Theta_+=\theta$ (solid line), and the Verlet method given by Eq. (38) (dashed line).

$$\Theta_{\pm}=\pm\cos^{-1}\left(1-\frac{\theta^2}{2}\right), \tag{38}$$

does not coincide with the exact solution, $\Theta_{\pm}^{\text{exact}}=\pm\theta$ (see this difference for Θ_+ in Fig. 5), and this is a source of the phase error in the Verlet scheme. The deviation (overestimate) becomes appreciable for $\theta\gtrsim 1$. Moreover, for $\theta>2$ the solutions $\mu_{\pm}$ become real, and one of them (μ_+) diverges exponentially. This restricts the possible values of θ to be $\theta<\theta_*=2$. Thus the maximum possible time step τ_* in the Verlet algorithm is

$$\tau_*\simeq\frac{2}{\omega_{\max}}, \tag{39}$$

with $\omega_{\max}$ being the maximum eigenfrequency in the spectrum.

Let us estimate the maximum phase error $\Delta\Theta_{\max}=\Theta_+(\theta_{\max})-\theta_{\max}$ (the estimate with Θ_- is similar) experienced by the fastest eigenmode, where $\theta_{\max}=\omega_{\max}\tau$. Suppose that the total time of the run containing N_τ steps is T. Then the total phase error $\epsilon_{\max}$, accumulated by the fastest eigenmode during the course of the simulation, is

$$\epsilon_{\max}=N_\tau\Delta\Theta_{\max}=\omega_{\max}T\frac{\Delta\Theta_{\max}}{\theta_{\max}}, \tag{40}$$

or

$$\frac{\Delta\Theta_{\max}}{\theta_{\max}}=\frac{\epsilon_{\max}}{\omega_{\max}T}. \tag{41}$$

In order to obtain concrete numbers for estimates (40) and (41), we have performed [2] simulations for the simplest harmonic atomic system, a perfect linear chain of atoms (see below) with the typical values $\omega_{\max}=2$ and $T=10\,000$. If we choose τ to be the standard value of about 1% of the period of the fastest eigenmode [18], i.e., $\theta_{\max}\approx 0.063$, then, from Eq. (40) we obtain an estimate $\epsilon_{\max}\approx 3.3$ which is not good at all. Conversely, if we demand reasonable values such as $\epsilon=10^{-3}$ and $\theta\approx 10^{-3}$, then the number of steps required is $N_\tau=2\times 10^7$. This means that the Verlet algorithm can be fast or moderately accurate, but not both. The FEM developed above is free of this drawback (see Table I below).

VI. IMPROVED VERLET METHOD

The reason for the great popularity of the Verlet algorithm, besides its simplicity, is related to the associated energy conservation, i.e., zero gain error (see Sec. V). However, the phase error in the Verlet algorithm can be actually not negligible at all if the parameters are not chosen properly. Proper choice of the parameters requires a very small time step, which is not very desirable for practical purposes. To avoid this drawback, we see the following way to improve the Verlet algorithm for harmonic systems.

Our aim in improving the Verlet scheme is to reduce the phase error while preserving the zero gain error. A straightforward way of doing this is to find an expression for μ [see Eqs. (35) and (36)], which is as close to μ^{exact} as possible. If $|\mu_{\pm}(\theta)|=1$, then $\mu_{\pm}(\theta)$ must be of the form $\mu_{\pm}(\theta)=f(\theta)\pm i\sqrt{1-f(\theta)^2}$. The function $f(\theta)$ for the original Verlet algorithm is given by Eq. (36). A logical improvement bringing it closer to Eq. (37) is

$$\begin{aligned}\mu_{\pm}(\theta)&=1-\frac{\theta^2}{2}+\frac{\theta^4}{24}\pm i\left[1-\left(1-\frac{\theta^2}{2}+\frac{\theta^4}{24}\right)^2\right]^{1/2}\\&\simeq 1\pm i\theta-\frac{\theta^2}{2}\mp\frac{i\theta^3}{6}+\frac{\theta^4}{24}\pm\frac{i\theta^5}{144}+\cdots,\end{aligned} \tag{42}$$

so that this expansion coincides with Eq. (37) up to and including terms $O(\theta^4)$. Rearranging Eq. (42) to eliminate the square root leads to a quadratic equation in μ (with the roots $\mu_{\pm}$):

TABLE I. Comparison of the performance of the simple Verlet (leap-frog) method and FEM for the time evolution of a δ-functional displacement perturbation in an ideal linear harmonic atomic chain.

Quantity	Verlet	Verlet	Verlet	FEM	FEM	FEM
Time step τ	0.01	0.1	1	1	10	4000
Number of steps N_τ	4×10^5	4×10^4	4×10^3	4×10^3	400	1
Order P for FEM	-	-	-	9	25	4105
CPU/$R$10 000 time (sec)	760	77.0	54.4	217	49.7	18.7
ϵ	5.5×10^{-2}	0.82	0.98	9.5×10^{-13}	8.4×10^{-13}	1×10^{-12}
ϵ_{gain}	-5×10^{-4}	-4×10^{-4}	2×10^{-3}	-5×10^{-13}	5×10^{-14}	-1×10^{-15}

$$\mu^2 - 2\left(1 - \frac{\theta^2}{2} + \frac{\theta^4}{24}\right)\mu + 1 = 0. \tag{43}$$

Comparison of Eqs. (43) and (34) shows that it corresponds to the triple recurrence

$$\mathbf{u}_{n+1} = 2\left(1 - \frac{\tau^2}{2}\mathbf{H} + \frac{\tau^4}{24}\mathbf{H}^2\right)\mathbf{u}_n - \mathbf{u}_{n-1}, \tag{44}$$

where for the sake of generality (the displacement vector need not be necessarily an eigenmode), the eigenvalue has been replaced by the dynamical matrix. The extension of the second term in Eq. (44) to higher orders in $(\sqrt{\mathbf{H}}\tau)$ shows that this is just a Taylor approximation to $\cos\sqrt{\mathbf{H}}\tau$, so that the improved triple Verlet recursion can be written as

$$\mathbf{u}_{n+1} = 2(\cos\sqrt{\mathbf{H}}\tau)\mathbf{u}_n - \mathbf{u}_{n-1}. \tag{45}$$

In a manner directly analogous to the FEM (see Sec. IV), we could approximate $(\cos\sqrt{\mathbf{H}}\tau)\mathbf{u}_n$ in Eq. (45) by a truncated Chebyshev polynomial expansion. This would produce a phase error more uniformly distributed over the spectrum of $\mathbf{H}$ (see below for a comparison of the phase errors produced by different methods).

This improved method has two drawbacks. First, the only way to obtain the velocity $\mathbf{v}_n$ is by differentiating $\mathbf{u}_n$ numerically. This is notoriously unstable for large τ. Therefore, it is necessary to run a separate recurrence to find $\mathbf{v}_n$, starting from $\mathbf{v}_0$ and $\mathbf{v}_1$. Second, the starting conditions for a simulation are usually supplied as $\mathbf{u}_0$ and $\mathbf{v}_0$, but $\mathbf{u}_1$ and $\mathbf{v}_1$ must be computed accurately before the triple recurrences can be launched. The best way to do this is, once again, to use the FEM itself. The only possible advantage of the improved Verlet method over the FEM is that it appears to guarantee energy conservation. However, due to the problem with launching, we found the energy conservation of the improved Verlet method to be no better than that of the FEM.

VII. PERFORMANCE OF THE FAST EVOLUTION METHOD: GREEN FUNCTION OF A LINEAR CHAIN

In order to compare the performance of the original Verlet and FEM schemes, we choose one of the simplest mechanical models, namely the linear one-dimensional (1D) harmonic atomic chain (see, e.g., Refs. [16,18], and references therein). Newton's equations of motion for such a model read

$$\frac{d^2u_n}{dt^2} = -\frac{\partial V}{\partial u_n}, \tag{46}$$

with the potential energy V given by

$$V = \tfrac{1}{2}\sum_n (u_n - u_{n+1})^2, \tag{47}$$

assuming that all masses $m_n = 1$ and spring constants $\kappa_n = 1$. The atoms in the chain are equidistantly positioned at $x_n = na$ $(n = 1, \ldots, N,\ a = 1)$ with periodic boundary conditions, and u_n are the displacements from these equilibrium positions. We have studied [2] the evolution of the δ-functional perturbation in this system described by the following initial conditions:

$$u_n(0) = \delta_n, \tag{48}$$

$$\dot{u}_n(0) = 0. \tag{49}$$

This choice of the initial conditions has been dictated by two reasons: (i) such a displacement pattern contains all the eigenmodes of the system, and (ii) the solution (the Green function) is known analytically (see, e.g., Ref. [16]), namely,

$$u_n(t) = J_{2n}(2t), \tag{50}$$

$$\dot{u}_n(t) = J_{2n-1}(2t) - J_{2n+1}(2t), \tag{51}$$

with $J_n(x)$ being the Bessel function.

The exact solution $\mathbf{u}^{\text{exact}}(t)$, given by Eq. (50), can be compared with the results of either the Verlet method, $\mathbf{u}^{\text{Ver}}(t)$, or FEM, $\mathbf{u}^{\text{FEM}}(t)$, thus allowing us to judge the quality of these approximate methods. The deviations of the approximate solutions from the exact one are characterized by the difference error $\epsilon = |\mathbf{u}^{\text{exact}} - \mathbf{u}|$ and the gain error $\epsilon_{\text{gain}} = (|\mathbf{u}|/|\mathbf{u}^{\text{exact}}|) - 1$ (with $\mathbf{u} = \mathbf{u}^{\text{FEM}}$ or $\mathbf{u} = \mathbf{u}^{\text{Ver}}$). It may seem strange that, although the Verlet method is supposed to have zero gain error, we obtained errors of the order of 10^{-3} from the simulation (see the values of ϵ_{gain} in Table I). This is due to the ''starting'' and ''stopping'' errors. They are related to the inevitable introduction of some gain errors when converting between the initial conditions $(\mathbf{u}_0, \mathbf{v}_0)$, the quantities in the Verlet recurrence $(\mathbf{u}_j, \mathbf{u}_{j+1})$, and the final quantities $(\mathbf{u}_{N_t}, \mathbf{v}_{N_t})$, even though the recurrence itself is gain free. In the case of the FEM, it is difficult to separate the gain and phase errors, and it is sufficient to consider the total error ϵ, which is typically very small, $\epsilon \sim 10^{-6} - 10^{-15}$ (see Table I).

Approximate solutions have been found numerically for $N = 10^4$ atoms and $t = 4000$ $(\omega_{\max} t = 8000)$. The results presented in Table I and Fig. 6 show that the FEM is much faster and much more precise [cf. Figs. 6(b) and 6(c)]. Indeed, the Verlet method can be either relatively fast but not precise (see the third column of Table I) or relatively precise but slow (see the first column Table I) in comparison with the always precise, very fast single-step (sixth column) and relatively fast, multiple-step (fourth column) FEM. As follows from Table I (cf. the fourth, fifth, and sixth columns), the strategy in accessing the best performance for the FEM is to choose the smallest number of integration steps, preferably just a single evolution step (sixth column), to the desired time t.

The dramatic increase in speed for the FEM is related to the relatively small number of matrix-vector operations needed as compared to the Verlet scheme. The leapfrog Verlet algorithm has one such operation per step, so that the total number of matrix-vector operations N_{mv} for time T is estimated to be $N_{\text{mv}}^{\text{Verlet}} \simeq 16\omega_{\max} T$ for a conventional choice of the parameters, $\tau = 0.01 \times 2\pi/\omega_{\max}$ and $N_{\text{mv}}^{\text{Verlet}} = N_\tau = T/\tau$. On the other hand, the number of matrix-vector operations per step for the FEM is $N_{\text{mv}}^{\text{FEM}} \simeq 2P - 1$. The maximum order

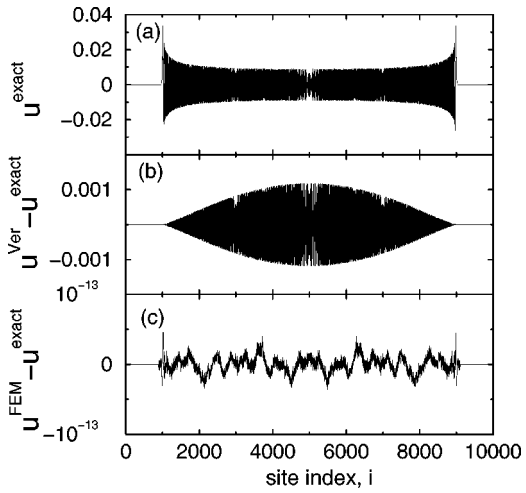

FIG. 6. Displacement pattern (the displacement u_i of atom i vs its equilibrium coordinate $R_i \equiv i$) for a δ-functional initial displacement perturbation at $i=5000$ in an ideal linear harmonic chain of 10^4 atoms at $\omega_{\max}t=4000$: (a) the exact solution, u_i^{exact}; (b) the difference between the approximate solution obtained by the Verlet method (with the integration time-step, $\tau=0.01$ and the number of steps, $N_\tau=4\times10^5$) and the exact solution, $u_i^{\text{Ver}}-u_i^{\text{exact}}$; (c) the difference between the approximate solution obtained by the FEM (with the integration time step $\tau=4\times10^3$, the number of steps, $N_\tau=1$ and the maximum order of the polynomials, $P=4105$) and the exact solution, $u_t^{\text{FEM}}-u_i^{\text{exact}}$.

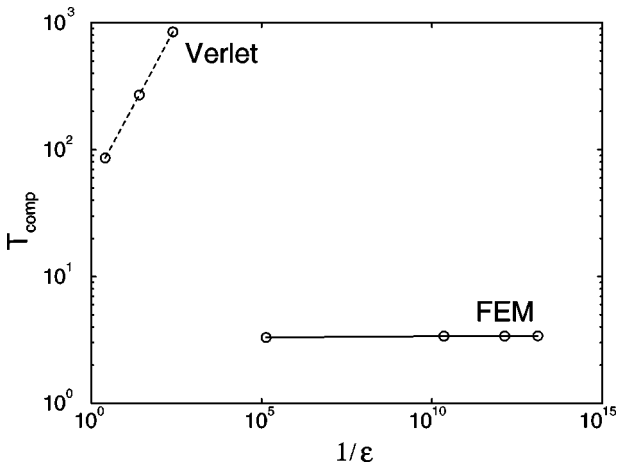

FIG. 7. Computational time T_{comp} (CPU/$R$10 000 in seconds), against the achieved difference error ϵ, for the FEM (solid line) and Verlet (dashed line) algorithms applied to describe the evolution of a δ-functional perturbation in a linear atomic chain, as described in the text. The parameters of the model are the following: number of atoms $N=10\,000$, total evolution time $T=500$, and maximum frequency $\omega_{\max}=2$.

of the Chebyshev polynomials is $P\simeq\chi\omega_{\max}T/\pi\sim\omega_{\max}T$ [see Eq. (25)], and bearing in mind that only one time step can be used to evolve the system for time T, we find that $N_{\text{mv}}^{\text{FEM}}=\zeta\omega_{\max}T/\pi$ with the numerical factor $\zeta\sim1$, i.e., approximately an order of magnitude faster than the Verlet scheme (as follows from Table I). Furthermore, whereas the Verlet method introduces an accumulated phase error of the order of 1 rad into the fastest eigenmodes, the Chebyshev method is essentially exact.

The advantage of the FEM can also be demonstrated by different scaling laws for the computational time with respect to a required error. In order to show this, let us find the dependence of the computational time, T_{comp}, on different values of the total phase error $\epsilon_{\max}$ [see Eq. (40)]. The computational time is proportional to the number of variables, N (for sparse matrices), and to the number of simulation steps, N_τ, i.e., $T_{\text{comp}}\propto NN_\tau$. The number of simulation steps, being the ratio of the total evolution time, T, to the length of the step, τ, can be estimated, with the use of Eq. (39), as $N_\tau=T/\tau\sim\omega_{\max}T/\theta_{\max}$. The phase $\theta_{\max}$ is related to the phase error per step, $\Delta\Theta_{\max}$, by the expansion in Eq. (38) for $\theta=\theta_{\max}\ll1$, i.e. $\theta_{\max}\sim\Delta\Theta_{\max}^{1/3}$, so that

$$N_\tau\sim\omega_{\max}T\Delta\Theta_{\max}^{-1/3}. \tag{52}$$

Bearing in mind relation (40), we can rewrite Eq. (52) as an implicit equation for N_τ,

$$N_\tau\sim\omega_{\max}T\left(\frac{\omega_{\max}}{N_\tau}\right)^{-1/3}, \tag{53}$$

the solution of which with respect to N_τ gives the proportionality $N_\tau\sim(\omega_{\max}T)^{3/2}\epsilon_{\max}^{-1/2}$. Therefore, the total computational time scales as the inverse square root of the error:

$$T_{\text{comp}}\propto N(\omega_{\max}T)^{3/2}\epsilon_{\max}^{-1/2}. \tag{54}$$

On the other hand, the total simulation time for a single step FEM can be estimated as $T_{\text{comp}}\propto NP(\epsilon)$, where the maximum number P of the polynomials in the expansion depends essentially logarithmically on ϵ [see Eq. (24)], which is much slower than the power-law dependence on ϵ for the Verlet algorithm given by Eq. (54) (see Fig. 7). Rough estimates of RAM and CPU time requirements for a vibrational problem in a 3D cubic lattice of 10^7 atoms are 10 Gb and 10 h/$R$10 000 for $\omega_{\max}t=10^2$.

VIII. APPLICATION OF THE FAST EVOLUTION METHOD TO WAVE-PACKET PROPAGATION

The behavior of waves propagating in disordered media is of widespread interest [7]. In particular, the problem of atomic-vibrational, plane-wave propagation in disordered systems [24], e.g., amorphous solids [25], and the concomitant Ioffe-Regel crossover between weak- and strong-scattering regimes [26], is of considerable importance in understanding the vibrational behavior of such materials. Wave-packet propagation [18,27] is pehaps of even greater interest, because it impacts directly on experimental quantities such as thermal conductivity of disordered materials [28]. In perfectly crystalline materials, wave packets can only propagate ballistically: the center of a launched wave packet moves relative to the medium, even though the width increases with time due to dispersion. In disordered materials, however, where disorder-induced scattering always occurs to a greater or lesser extent, as well as ballistic motion, wave packets can evolve in time in two other completely

different ways. The evolution may be diffusive (i.e., a random-walk-like behavior). After ballistic propagation of a launched wave packet over a distance of a few times the mean free path, multiple scattering becomes significant, and a diffusive behavior occurs, in which the center of the wave packet remains stationary, while the width increases as the square root of elapsed time. For a sufficiently large degree of disorder, a wave packet may even become localized (when the majority of the eigenmodes making up the wave packet are localized), in which both the wave packet mean position and width become time independent. However, simulation of wave-packet propagation by using, e.g., the Verlet algorithm [18], is very unsatisfactory, as discussed in Sec. V. In this section, we consider the use of Chebyshev-polynomial FEM to simulate wave-packet propagation in a model disordered medium, as an example of the applicability and usefulness of this approach.

The system studied was a harmonic fcc lattice containing $N\times N\times N$ atoms with periodic boundary conditions ($N=120$) connected by springs characterized by spring constants κ. Disorder was introduced in the model in the form of cellular (lattice) disorder via a distribution $\rho(\kappa)$ of spring constants. The force-constant probability distribution chosen was a box (uniform) distribution, centered at a value κ_0, and with a width $\Delta\kappa$, i.e., $\kappa\in[\kappa_0-\Delta\kappa/2,\kappa_0+\Delta\kappa/2]$. This type of model reproduces essential features of the vibrational behavior of real amorphous solids, such as the low-frequency boson peak in the vibrational density of states [29,30].

In order to investigate the time evolution of the vibrational wave packet, first we have to construct it, i.e., to specify the initial conditions of the problem. There is a certain degree of freedom in choosing the shape of an initial wave packet. Here we consider only spatially Gaussian wave packets, but even for these there are a number of adjustable parameters. Such wave packets can be described by their amplitude $|\mathbf{U}|$, mean position $\mathbf{R}_0$, mean wave vector $\mathbf{k}_0$, a ''width'' tensor $\mathbf{W}_0$, and for vibrational excitations, a polarization (contained in the amplitude vector $\mathbf{U}$, a phase velocity $\mathbf{v}_p$, and a group velocity $\mathbf{v}_g$. Below we study only spherically symmetric wave packets, with $\mathbf{W}_0=W_0\mathbf{I}$, where W_0 is the width of the wave packet along any direction which obeys the restrictions $a\ll W_0\ll L$, where a is the lattice unit cell size and L is the box size. Obviously, the larger W_0 is, the smaller the spread of the wave packet in reciprocal $\mathbf{k}$ space, and vice versa. Therefore, the initial wave packet can be written in the form.

$$|\mathbf{u}_0\rangle=\mathrm{Re}\sum_n^N \mathbf{U}\exp\left[\mathrm{i}\mathbf{k}_0\cdot\mathbf{R}_n-\frac{1}{2}(\mathbf{R}_n-\mathbf{R}_0)\mathbf{W}_0^{-2}(\mathbf{R}_n-\mathbf{R}_0)\right]|n\rangle \tag{55}$$

for the initial displacement vector (n runs over all the atoms in the system), and

$$|\mathbf{v}_0\rangle=\mathrm{Re}\sum_n^N \mathbf{U}[\mathbf{v}_g\mathbf{W}_0^{-2}(\mathbf{R}_n-\mathbf{R}_0)-\mathrm{i}\mathbf{v}_p\cdot\mathbf{k}_0]\times\exp\left[\mathrm{i}\mathbf{k}_0\cdot\mathbf{R}_n-\frac{1}{2}(\mathbf{R}_n-\mathbf{R}_0)\mathbf{W}_0^{-2}(\mathbf{R}_n-\mathbf{R}_0)\right]|n\rangle \tag{56}$$

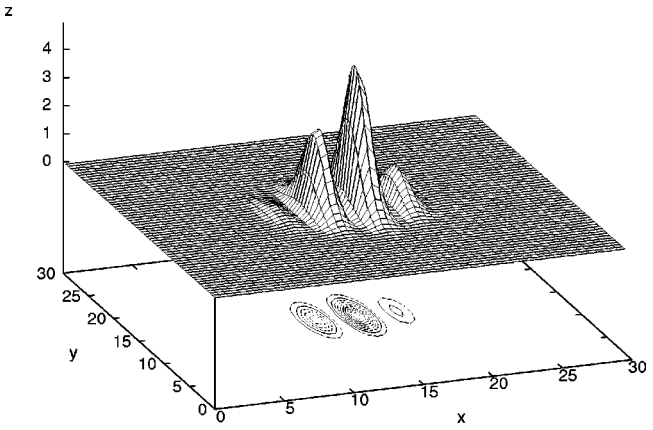

FIG. 8. Visualization of a typical initial longitudinal wave packet created at the body center of the simulation box containing $30\times30\times30$ cubic nonprimitive unit cells (four atoms per unit cell) of the fcc lattice. The squared displacements $z=u_{xy}^2$ are shown, projected onto the $x-y$ plane, $u_{xy}^2\simeq\Sigma_n|\mathbf{u}_n|^2\delta(x-R_{nx})\,\delta(y-R_{ny})$, vs $x-y$ coordinates of the unit cells. The parameters describing the initial Gaussian wave packet at $t=0$ are the position $\mathbf{R}_0=(15,15,15)$, the Gaussian width tensor $\mathbf{W}_0=3\mathbf{I}$, the average wave vector $\mathbf{k}_0=(1,0,0)$, the phase velocity $\mathbf{v}_p=(0.64,0,0)$, the group velocity $\mathbf{v}_g=(0.64,0,0)$, and the polarization vector $\mathbf{U}=(1,0,0)$.

for the initial velocity vector. The atomic velocities $|\mathbf{v}_0\rangle$ determine the direction of travel of the wave packet, and to calculate them requires a knowledge of both the phase and group velocities. Failure to take these into account correctly results in a wave that (e.g., in one dimension) splits into two parts, traveling in opposite directions. In order to eliminate such unwanted reflections of the wave packet completely, it is necessary to take higher-order derivatives of the dispersion relation $\omega(k)$ into account (the group velocity being just the first derivative). A typical initial wave packet, which was propagated by the FEM, is shown in Fig. 8.

Once the initial wave packet is constructed, it can be propagated forward in time using the FEM. Before doing this, first let us specify the physical characteristics of the wave packet we would like to follow. These are the average position $\langle\mathbf{R}(t)\rangle$ of the wave packet, and its width $W(t)$. Their definitions for the electron case are obvious and are related to the probabilities $P_n(t)=|\langle n|\psi(t)\rangle|^2$ to find an electron on site n, so that

$$\langle\mathbf{R}(t)\rangle=\frac{\sum_n P_n(t)\mathbf{R}_n}{\sum_n P_n(t)}. \tag{57}$$

The width of the wave packet can be defined via a variance tensor $\mathbf{V}$,

$$\mathbf{V}=\langle\mathbf{R}(t)\mathbf{R}^T(t)\rangle-\langle\mathbf{R}(t)\rangle\langle\mathbf{R}^T(t)\rangle \equiv\frac{\sum_n P_n(t)\mathbf{R}_n\mathbf{R}_n^T}{\sum_n P_n(t)}-\langle\mathbf{R}(t)\rangle\langle\mathbf{R}^T(t)\rangle \tag{58}$$

($\mathbf{R}^T$ stands for a transposed D-dimensional vector) as a square root of its trace,

$$W=\sqrt{D^{-1}\,\mathrm{Tr}\,\mathbf{V}}. \tag{59}$$

These definitions hold true for the vibrational wave packet as well, but the meaning of the probability P_n is different. In the case of atomic vibrations, the value P_n is associated with a local vibrational energy [18] and one of the possible ways of its definition is the following [27]:

$$P_n=\tfrac{1}{2}|\langle n|\mathbf{v}(t)\rangle|^2+\tfrac{1}{2}\,\langle \mathbf{u}(t)|n\rangle\langle n|\mathbf{H}|\mathbf{u}(t)\rangle. \tag{60}$$

Here $\mathbf{H}$ stands for the dynamical matrix with elements, $\mathbf{H}_{nn'}$, which are $D\times D$ matrices [16], $H_{n\alpha,n'\beta}=(1/2)(\kappa_{nn'}/\sqrt{m_n m_{n'}})[(\mathbf{R}_m-\mathbf{R}_n)_\alpha(\mathbf{R}_m-\mathbf{R}_n)_\beta/|\mathbf{R}_m-\mathbf{R}_n|^2]$, with $\kappa_{nn'}$ denoting the spring constant between atoms n and n' having masses m_n and $m_{n'}$; the indices α and β run over the Cartesian coordinates.

As a test of the efficiency of the Chebyshev-polynomial-based FEM as applied to wave-packet propagation, we have investigated the time-evolution behavior of free [18] (and driven [27]) atomic-vibrational wave packets in a fcc disordered lattice characterized by different values of disorder (different $\Delta\kappa$) and also electron wave-packet propagation in the same lattice described by the Anderson-model Hamiltonian [5]. Below, we discuss only the results for free vibrational wave-packet propagation. Initial free longitudinal-acoustic (*LA*)-like vibrational wave packets were generated, with average wave vector and polarization in, say, the x direction. The phase and group velocities required [see Eq. (57)] were obtained from the $\omega(k)$ dispersion relation calculated for the fcc crystal: the LA branch is almost linear between the k values (0,0,0) and $(\pi/a,0,0)$.

The results of these FEM simulations for wave packets characterized by different initial average wave vectors $\mathbf{k}_0$, and propagating in structures with different degree of disorder, $\Delta\kappa/\kappa_0$, are presented in Figs. 9–11. A wave packet characterized by a relatively small initial average wave vector, $\mathbf{k}_0=(1,0,0)$, propagates in crystalline and not very strongly disordered media ($\Delta\kappa/\kappa_0=0$ and 0.5, respectively) in the ballistic regime [see Figs. 9(a) and 9(b)]. Indeed, both the average position of the wave packet and its width scale almost linearly with time, $\langle R_x(t)\rangle\propto t$ and $W(t)\propto t$ [see Figs. 11(a) and 11(d)]. The ''wraparound'' effects are evident in the wave-packet profile due to reflections from the boundaries of the simulation box. Increasing the disorder to $\Delta\kappa/\kappa_0=1.0$ results in a deviation from ballistic behavior and a start of the crossover to the diffusive regime, i.e., the time dependence of the average position of the package begins to deviate from linearity [see the dot-dashed line in Fig. 11(a)] and the shape of the packet is changed as well; it is appreciably broadened and elongated, see Fig. 9(c)].

The diffusive character of propagation is enhanced with increasing both the initial average wave vector and the degree of disorder. Indeed, the wave packet characterized by $\mathbf{k}_0=(2,0,0)$ propagates through the disordered medium with $\Delta\kappa/\kappa_0=2.0$ in the diffusive regime [see Fig. 10(c)]. In this regime, the wave packet average position is time independent, ($\langle R_x(t)\rangle\simeq$const, and the wave-packet width scales with time as ($W\propto t^{1/2}$) [see the dot-dashed lines in Figs. 11(b) and 11(e)]. At higher values of $\mathbf{k}_0$, the diffusive behavior is even more pronounced [see Figs. 11(c) and 11(d)].

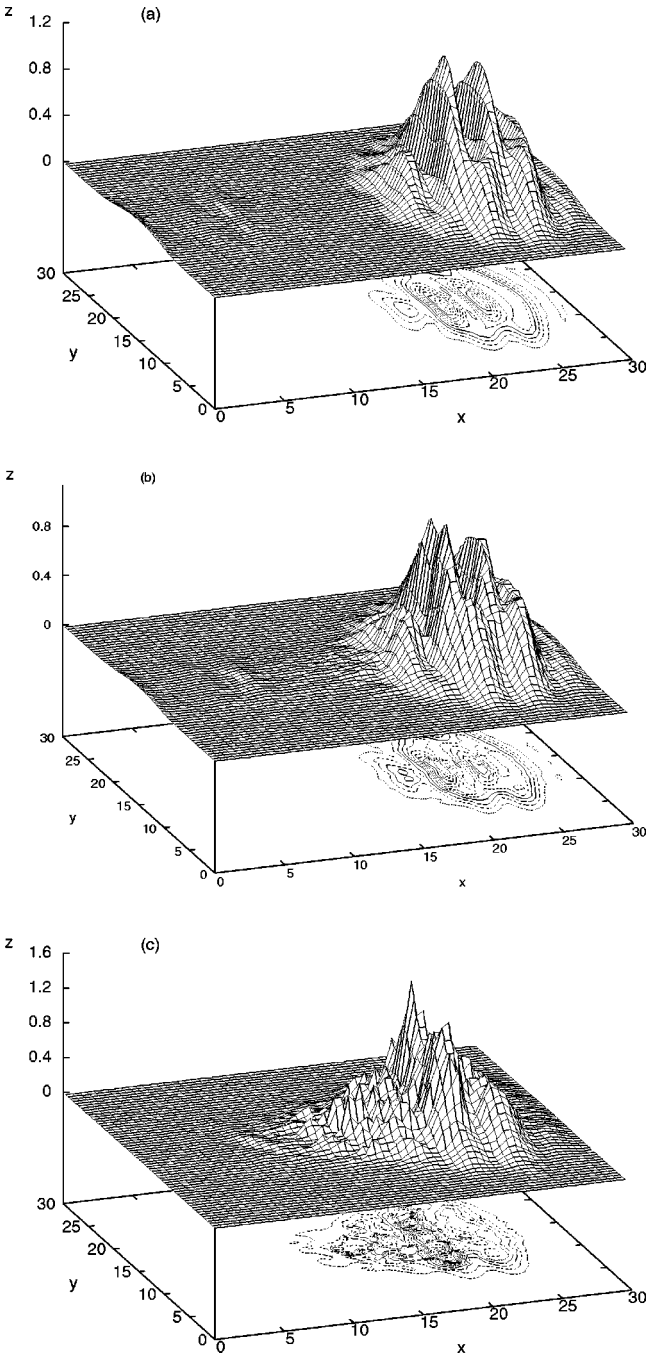

FIG. 9. Visualization of the time evolution of a free longitudinal vibrational wave packet with an initial average wave vector $\mathbf{k}_0=(1,0,0)$ in a $30\times30\times30$ unit cell (cubic nonprimitive) fcc lattice, calculated using the FEM at $t=15$ in structures characterized by different degrees of disorder. (a) The wave packet in a disorder-free ($\Delta\kappa=0$) crystalline lattice. The extra structure in the wave packet shape is due to boundary-induced wraparound effects. (b) and (c). The wave packet in a force-constant-disordered lattice with $\Delta\kappa/\kappa_0=0.5$ and $\Delta\kappa/\kappa_0=1.0$, respectively. The axis notations and the parameters of the initial wave packet are the same as in Fig. 8.

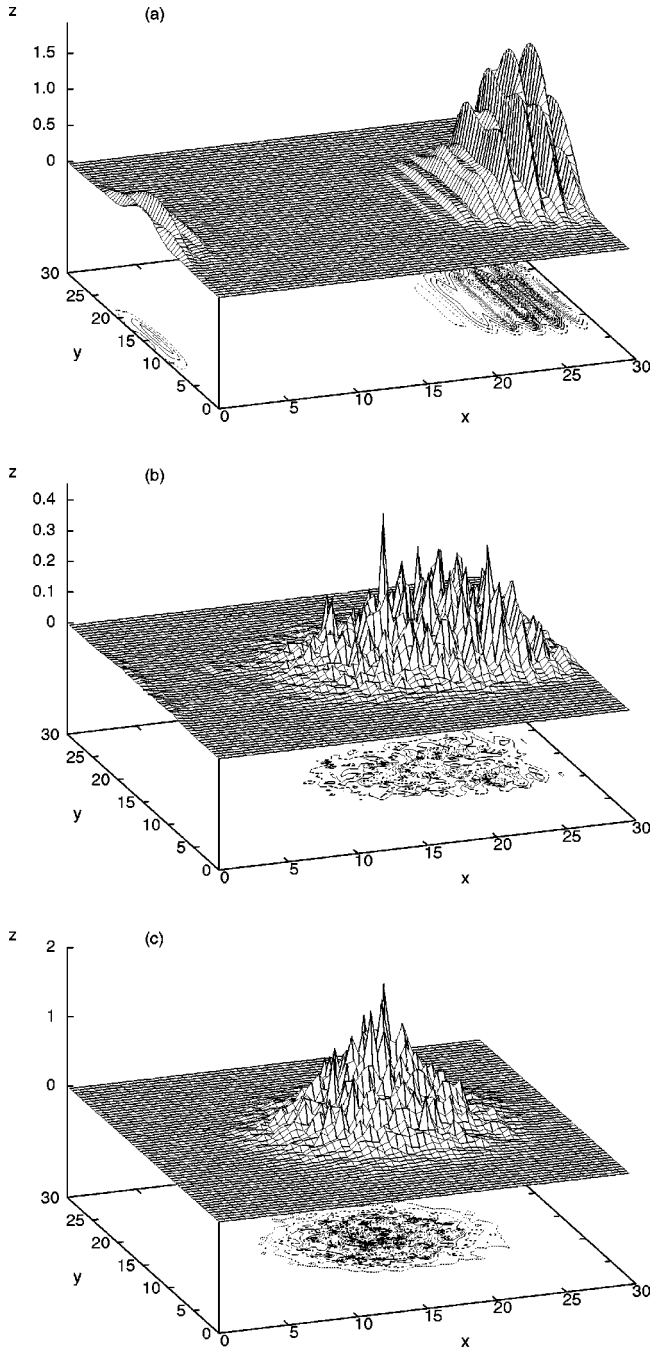

FIG. 10. Visualization of the time evolution of a free longitudinal vibrational wave packet with an initial average wave vector $\mathbf{k}_0 = (2,0,0)$ in models characterized by different degrees of disorder: (a) $\Delta\kappa=0$, (b) $\Delta\kappa=0.5$, and (c) $\Delta\kappa=1.0$. The other parameters are the same as in Figs. 8 and 9.

The other effect which is typical of wave-packet propagation in disordered media is a mixture of polarizations [25] which is due to disorder-induced hybridization between different branches [30]. Indeed, although the initial wave packet launched was purely longitudinal in character, the time-evolution simulations show that disorder-induced longitudinal-transverse scattering occurs for the propagation in the force-constant-disordered lattice, and both longitudinal and transverse components are present in the wave packet after a certain time t (Fig. 12).

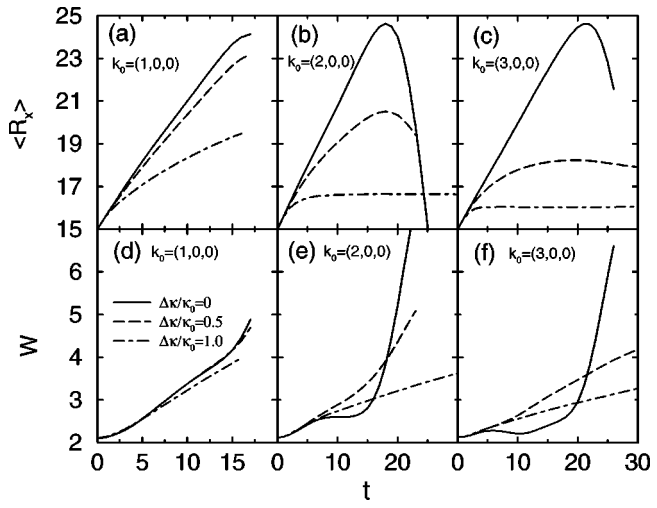

FIG. 11. Trajectories of the average positions [(a)–(c)] and widths [(d)–(f)] of longitudinal vibrational wave packets propagating in a lattice containing varying degrees of force-constant disorder $\Delta\kappa/\kappa_0$, as marked, and for three initial average wave vectors $\mathbf{k}_0$, as marked (the other parameters are as in Figs. 8 and 9). The turnover in the curves is due to the boundary-induced wraparound effects in Figs. 9 and 10.

IX. CONCLUSIONS

We have developed a Chebyshev-polynomial-based fast-evolution method for classical and quantum linear dynamical systems. The method requires the existence of eigenfunctions and eigenvalues of the problem, but does not require them to be computed explicitly. It uses only the interaction operator in matrix form, and initial conditions. The key point of the method is related to a polynomial expansion of the formal solution at an arbitrary time t. These polynomials are defined in terms of the operators (matrices), but the coefficients are scalars depending on time and are independent of the type of variables for the polynomials. The fast-evolution method is computationally efficient, and can be used for large systems containing up to 10^7 particles. It differs in principle from the standard time-integration schemes (e.g., Verlet), and appears to be much more accurate and faster.

The fast-evolution method is general and applicable to many physical problems. We have investigated the performance of the method by analyzing a classical one-dimensional atomic harmonic system. Extension of the method to the solution of the diffusional and wave equations is also quite straightforward. We have also demonstrated the use of this method to the problem of wave-packet propagation in disordered structures.

ACKNOWLEDGMENTS

The authors are grateful to Professer T. Nakayama for drawing their attention to Ref. [10]. We also thank Jon Ludlam and Gana Natarajan for their assistance in the computations. Y.L.L. is grateful to Trinity College, Cambridge, for the provision of a summer studentship.

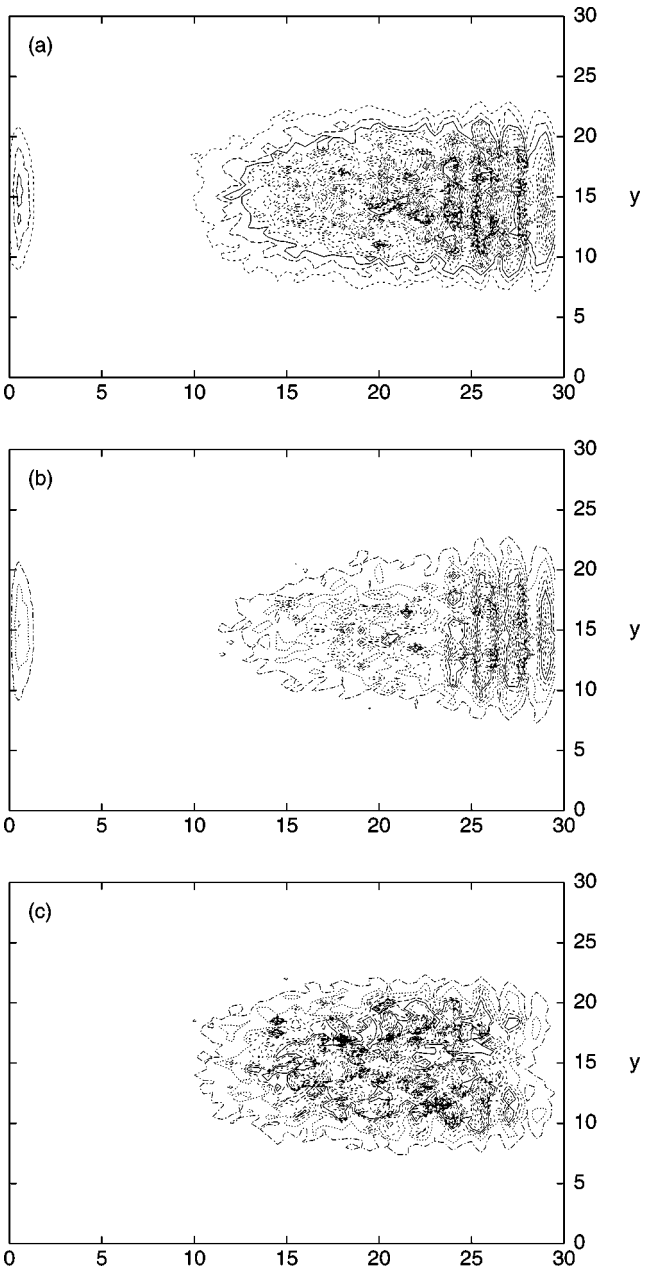

FIG. 12. Longitudinal-transverse scattering in the time evolution (at $t=15$) of an initially longitudinal vibrational wave packet [$\mathbf{k}_0=(2,0,0)$ (the other parameters are as in Fig. 8)], propagating in a force-constant disordered $30\times30\times30$ unit-cell fcc lattice ($\Delta\kappa/\kappa_0=0.5$). Contour plots of the squared displacements projected on the $x-y$ plane (as in Fig. 8) are shown. (a) Total displacements. (b) Longitudinal displacements. (c) Transverse displacements.

APPENDIX

In this Appendix we demonstrate how the coefficients $a_p(t)$ and $b_p(t)$ in expansions (20) and (21) can be evaluated. Let us consider the functions $A(\mathbf{H}^s)$ and $B(\mathbf{H}^s)$ defined in terms of the matrices in the site representation. If the coefficients α_i in Eq. (9) are real, then below we understand $A(\mathbf{H}^s)$ and $B(\mathbf{H}^s)$ as their real parts. In the case of complex coefficients, the real and imaginary parts of these functions can be treated separately, as demonstrated at the end of Sec. IV. Transformation to the eigenmode basis, e.g., $\mathbf{E}^{-1}A(\mathbf{H}^s)\mathbf{E}=A(\mathbf{H}^e)\simeq\Sigma_{p=0}^{P-1}a_p(t)T_p((\mathbf{H}^e)')$, reduces the problem to polynomials defined in terms of scalars, $T_p(\lambda_m)$, i.e., in terms of the diagonal elements of the matrix $\mathbf{H}^e$. This means that the coefficients $a_p(t)$ and $b_p(t)$ can be evaluated from the following relations for the functions defined in terms of the scalar variables:

$$A(\lambda;t)\simeq\sum_{p=0}^{P-1}a_p(t)T_p(\lambda'), \tag{A1}$$

$$B(\lambda;t)\simeq\sum_{p=0}^{P-1}b_p(t)T_p(\lambda'), \tag{A2}$$

where λ' is a scaled and shifted version of $\lambda\in[\lambda_{\min},\lambda_{\max}]$ designed to fall within the range $[-1,1]$,

$$\lambda'=\frac{2\lambda}{\lambda_{\max}-\lambda_{\min}}-\frac{\lambda_{\max}+\lambda_{\min}}{\lambda_{\max}-\lambda_{\min}}, \tag{A3}$$

which is similar to Eq. (19).

Consider, for example, the expansion of $A(\lambda)$:

$$A(\lambda;t)\simeq\sum_{p=0}^{P-1}a_p(t)T_p(\lambda')\equiv\sum_{p=0}^{P-1}a_p(t)\cos(p\cos^{-1}\lambda'). \tag{A4}$$

In order to find the coefficients $a_p(t)$, it is convenient to sample the continuous variable $\phi=\cos^{-1}(\lambda')$ at P discrete points, and introduce a new discrete variable q defined by the relation $q=P\phi/\pi$, so that $q=0,\ldots,P-1$. Multiplying Eq. (A4) by the polynomials $T_{p'}(q)$, and using the orthogonality property

$$\sum_{q=0}^{P-1}T_p(q)T_{p'}(q)=\frac{1}{2}(1+\delta_{p,0})P, \tag{A5}$$

we obtain the following relation for $a_p(t)$:

$$a_p(t)=\frac{2}{(1+\delta_{p,0})P}\sum_{q=0}^{P-1}A\times\left[\left(\bar{\lambda}+\Delta\lambda\cos\left(\frac{\pi q}{P}\right)\right);t\right]\cos\left(\frac{\pi pq}{P}\right), \tag{A6}$$

with $\bar{\lambda}=(\lambda_{\max}+\lambda_{\min})/2$ and $\Delta\lambda=(\lambda_{\max}-\lambda_{\min})/2$. This expression is in fact a discrete cosine transform, and can be easily computed using the FFT algorithm. The coefficients $b_p(t)$ are calculated similarly, exchanging the function $A(\lambda;t)$ for $B(\lambda;t)$.

[1] D. Frenkel and B. Smit, *Understanding Molecular Simulation from Algorithms to Applications* (Academic, New York, 1996).
[2] Y. L. Loh, S. N. Taraskin, and S. R. Elliott, Phys. Rev. Lett. **84**, 2290 (2000).
[3] Y. L. Loh, S. N. Taraskin, and S. R. Elliott, Phys. Rev. Lett. **84**, 5028 (2000).
[4] T. Odagaki and M. Lax, Phys. Rev. B **24**, 5284 (1981).
[5] B. Kramer and A. MacKinnon, Rep. Prog. Phys. **56**, 1469 (1993).
[6] T. Brandes, B. Huckestein, and L. Schweitzer, Ann. Phys. (Leipzig) **5**, 633 (1996).
[7] *Scattering and Localization of Classical Waves in Random Media*, edited by P. Sheng (World Scientific, Singapore, 1990).
[8] S. N. Taraskin and S. R. Elliott, J. Phys.: Condens. Matter **11**, A219 (1999).
[9] R. N. Silver and H. Röder, Phys. Rev. E **56**, 4822 (1997).
[10] Y. Okamoto and H. J. Maris, Comput. Phys. Commun. **76**, 191 (1993).
[11] H. Tal-Ezer and R. Kosloff, J. Chem. Phys. **81**, 3967 (1984).
[12] R. Kosloff, Annu. Rev. Phys. Chem. **45**, 145 (1994).
[13] R. Chen and H. Guo, Comput. Phys. Commun. **119**, 19 (1999).
[14] C. Leforestier *et al.*, J. Comput. Phys. **94**, 59 (1991).
[15] L. D. Landau and E. M. Lifshitz, *Quantum Mechanics, Non-Relativistic Theory* (Pergamon, Oxford, 1963).
[16] A. A. Maradudin, E. W. Montroll, G. Weiss, and I. P. Ipatova, *Theory of Lattice Dynamics in the Harmonic Approximation* (Academic, New York, 1971).
[17] C. Kittel, *Quantum Theory of Solids* (Wiley, New York, 1963).
[18] P. B. Allen and J. Kelner, Am. J. Phys. **66**, 497 (1998).
[19] G. H. Golub and C. F. van Loan, *Matrix Computations* (Johns Hopkins University Press, Baltimore, 1996).
[20] K. Yakubo, T. Nakayama, and H. J. Maris, J. Phys. Soc. Jpn. **60**, 3249 (1991).
[21] I. K. Zharekeshev and B. Kramer, Phys. Rev. Lett. **79**, 717 (1997).
[22] M. F. Thorpe and S. W. de Leeuw, Phys. Rev. B **33**, 8490 (1986).
[23] T. Nakayama and H. Shima, Phys. Rev. E **58**, 3984 (1998).
[24] P. Tong, B. Li, and B. Hu, Phys. Rev. B **59**, 8639 (1999).
[25] S. N. Taraskin and S. R. Elliott, Phys. Rev. B **61**, 12 017 (2000).
[26] S. N. Taraskin and S. R. Elliott, Phys. Rev. B **61**, 12 031 (2000).
[27] P. Sheng, M. Zhou, and Z. Q. Zhang, Phys. Rev. Lett. **72**, 234 (1994).
[28] P. B. Allen and J. L. Feldman, Phys. Rev. B **48**, 12 581 (1993).
[29] W. Schirmacher, G. Diezemann, and C. Ganter, Phys. Rev. Lett. **81**, 136 (1998).
[30] S. N. Taraskin, Y. L. Loh, G. Natarajan, and S. R. Elliott, Phys. Rev. Lett. **86**, 1255 (2001).